A Hierarchical Classification of Experimental Liver Carcinogenesis by Texture Analysis Using Laws Convolution Matrices

S.Baheerathan[1,2], F. Albregtsen[1], K. Yogesan[1,2], and H. E. Danielsen[2]

[1]Image Processing Laboratory
Department of Informatics, University of Oslo, Norway

[2]Department of Pathology
The Norwegian Radium Hospital, Oslo, Norway

Abstract

Chromatin structure in cell nuclei both reflects and partly controls genetic functions. Therefore, studies of chromatin structure during carcinogenesis is important. Texture is also one of several properties by which human beings perceive images, and it could be an important property for the classification of biomedical images. The objective of this study was to examine the early detection of malignancy by using the texture estimators of Laws on mice liver cell nuclei. Therefore, four groups of liver cells, *normal, regenerating, premalignant* and *malignant* were studied. The material was divided into a training set and an independent test set, where the training set had 20 animals, 5 from each of the 4 groups, and the test set had 10 animals from the *premalignant* group and 6 from the *malignant*. Digital transmission electron micrographs (TEM) of approximately 100 cell nuclei from each sample were used to extract texture features based on nine 3×3 Laws matrices. A linear discrimination model was used for statistical analysis, and a hierarchical classification (HC) system was followed to discriminate each group. The performance of the best combinations of three features was tested. At the first step of HC, all the *malignant* samples were correctly classified (100%). Then at the next step, all the *normal* samples were discriminated (100%) from the *regenerating* and *premalignant*. At the third step, the correct classification between the *regenerating* and *premalignant* was 100%. The above results demonstrated the value of using Laws texture features and employing a HC system in diagnosis of tumor pathology.

1 Introduction

Chromatin structure has traditionally been of major importance as a diagnostic clue in tumor pathology. The way chromatin compacts in a cell nucleus and what that compaction reflects in nuclear texture, suggest us to use texture estimation to discriminate between malignant and normal cells.

Previously, first-order statistics and morphological measurements were used on TEM images of cell nuclei to describe the differences between normal and malignant mouse liver cells [5]. Several texture estimators (LIT-SNN, GLCM, GLRLM, Fractal dimension) have also been tested and compared for discrimination of these images ([1], [2]).

When the quest of early detection of malignancy arises, it is necessary to include the group of *premalignant* (or *nodule*). Since the *premalignant* and *malignant* cells have higher proliferation, separation between the *normal* group and the above two groups might be due to proliferation, and not carcinogenesis. So, as a positive control for proliferation, a fourth group of *regenerating* liver (damaged liver which grow or regenerate back to it old size and capacity) was included ([6], [11], [4], [9], and [12]).

The aim of this paper was to use Laws [8] features as quantitative measures of chromatin texture on TEM images of cell nuclei, and use these features to discriminate between early as well as later stages of liver carcinogenesis by following a hierarchical classification system (HC).

2 Materials

2.1 Preparation of Liver Sections and TEM

All specimens were taken from C3H/HeJ male mice and cut into blocks less than $1mm$ in size and fixed with 2% glutaraldehyde in $0.1M$ cacodylate buffer with $0.1M$ sucrose, pH 7.4 at 4^0C for 48 hours ([5]). They were rinsed overnight in $0.1M$ cacodylate buffer with $0.2M$ sucrose and post-fixed with 1% osmium tetroxide in $0.1M$ cacodylate buffer with $0.1M$ sucrose, pH 7.4, at 20^0C. Thereafter the material was dehydrated in graded ethanol, rinsed 3 times in propylenoxide and embedded in Epon. Ultra-thin sections were stained first with uranyl-acetate and then lead citrate, and studied at a magnification of 2500 in a JEOL EX1200 transmission electron microscope at 60kv with a $20\mu m$ aperture. The cell images were recorded on Kodak 4489 EM photographic film and were digitized using a Sony CCD video camera(XC-77CE, Japan), which lead to total magnification of 7500. The digitized images are $512 \times 512 \times 8$ bits, and the image resolution is 39 nm per pixel.

The present study consisted of four different groups of cell nuclei, *normal, regenerating, premalignant* and *malignant*, and two sets of material, one training set and one independent test set. The training set had 20 animals, 5 from each of the 4 groups, and approximately 100 cell nuclei from each sample.

The main aim in examination of early stages of malignancy is discriminating the *premalignant* group from the rest of the groups. So, the independent test set had 10 animals from the *premalignant* group, 6 from the *malignant*, and approximately 100 cell nuclei from each sample. Thus, a total of 3600 nuclei were analyzed in this study. Figure 1 shows four samples of cell nuclei.

2.2 Preprocessing

The original data may contain some noise. The results of an image classification based on texture might improve if random noise is removed from the input data. In our study we used a 3×3 *median* filter to remove noise. Cell-nucleus segmentation, by manual outlining, was used since we are only interested in texture within the cell nuclei. All segmented images were scaled to the same mean (127.5) and standard deviation (50.0), to correct for possible variations in the light conditions due to e.g. the photographic processes.

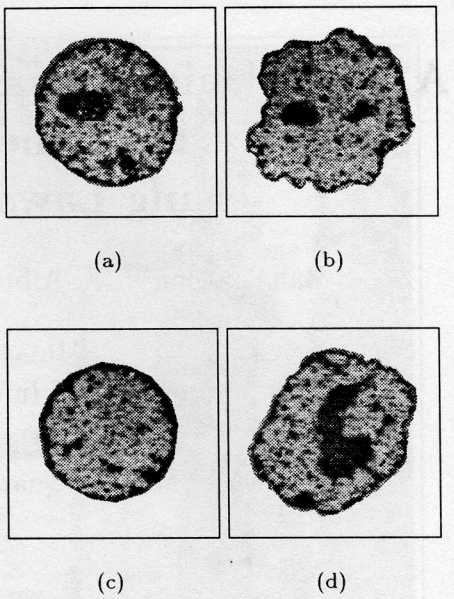

Figure 1: *Four samples from the liver cell data base, showing normal (a), regenerating (b), premalignant (c) and malignant (d)cell nuclei.*

3 Texture Estimators

Laws [8] proposed a methodology for image segmentation using texture analysis, which has two steps. In the first step an image is convolved with a mask, and in the second the local variance is computed over a moving window. The masks he proposed are small, separable and simple, and can in turn be derived from three simple vectors of length three, L3 = (1 2 1), E3 = (-1 0 1), S3 = (-1 2 -1). These vectors represent the one dimensional operations of center weighted local averaging, symmetric differencing (edge detection) and second differencing.

Nine 3×3 Laws masks can be generated by convolving 3×1 column vectors with 1×3 row vectors.

$$\underset{\text{L3L3}}{\begin{bmatrix} 1 & 2 & 1 \\ 2 & 4 & 2 \\ 1 & 2 & 1 \end{bmatrix}} \quad \underset{\text{L3E3}}{\begin{bmatrix} -1 & 0 & 1 \\ -2 & 0 & 2 \\ -1 & 0 & 1 \end{bmatrix}} \quad \underset{\text{L3S3}}{\begin{bmatrix} -1 & 2 & -1 \\ -2 & 4 & -2 \\ -1 & 2 & -1 \end{bmatrix}}$$

$$\underset{\text{E3L3}}{\begin{bmatrix} -1 & -2 & -1 \\ 0 & 0 & 0 \\ 1 & 2 & 1 \end{bmatrix}} \quad \underset{\text{E3E3}}{\begin{bmatrix} 1 & 0 & -1 \\ 0 & 0 & 0 \\ -1 & 0 & 1 \end{bmatrix}} \quad \underset{\text{E3S3}}{\begin{bmatrix} 1 & -2 & 1 \\ 0 & 0 & 0 \\ -1 & 2 & -1 \end{bmatrix}}$$

$$\underset{\text{S3L3}}{\begin{bmatrix} -1 & -2 & -1 \\ 2 & 4 & 2 \\ -1 & -2 & -1 \end{bmatrix}} \quad \underset{\text{S3E3}}{\begin{bmatrix} 1 & 0 & -1 \\ -2 & 0 & 2 \\ 1 & 0 & -1 \end{bmatrix}} \quad \underset{\text{S3S3}}{\begin{bmatrix} 1 & -2 & 1 \\ -2 & 4 & -2 \\ 1 & -2 & 1 \end{bmatrix}}$$

Most studies employing the Laws masks are related to image segmentation or pixel-wise classification of an image. To our knowledge, no one has worked with Laws texture features for classifing a whole image, particularly on TEM images. In this paper, we have used the nine Laws masks to extract features from the cell nucleus region R. First, an image was convolved with a 3×3 mask, such that the mask was totally inside the cell nucleus. Then, from the convolved image $L(i,j)$ the following five texture features were computed inside the cell-nucleus region R.

- Mean:

$$\mu_L = \frac{1}{N} \sum_i \sum_j L(i,j), \quad (i,j) \in R$$

- Standard deviation:

$$\sigma_L = \frac{1}{N} \sum_i \sum_j (L(i,j) - \mu_L)^2, \quad (i,j) \in R$$

- Absolute average:

$$\text{AA} = \frac{1}{N} \sum_i \sum_j |L(i,j)|, \quad (i,j) \in R$$

- Positive average:

$$\text{PA} = \frac{1}{N_p} \sum_i \sum_j L(i,j), \quad (i,j) \in R, \; L(i,j) \geq 0$$

- Negative average :

$$\text{NA} = \frac{1}{N_n} \sum_i \sum_j L(i,j), \quad (i,j) \in R, \; L(i,j) < 0$$

where N, N_p, and N_n correspond to the total, positive, and negative number of pixels in R.

Among the 9 Laws masks there are 3 mask pairs that are transposes of each other (L3E3 and E3L3, L3S3 and S3L3, E3S3 and S3E3). Since these masks give the same information in different (ortogonal) directions, the features obtained from the masks of pair were combined to give an average feature, independent of direction.

Thus, we ended up with six masks, as given in Table 1, where the first three were applied without transpose, and the last three with transpose. A total of 30 features, 5 from each of the six masks, were extracted from each single cell image. An animal was represented in feature space by averaging each feature over the number of cells representing it.

Notation	Mask
M1	L3L3
M2	E3E3
M3	S3S3
M4	L3E3
M5	L3S3
M6	E3S3

Table 1: *The notation of the masks which have been selected after considering the directional independence.*

4 Statistical Analysis

A linear discrimination model from the SPSS/PC+ statistical package (SPSS, Inc., Chicago, Illinois, U.S.A) was used in this analysis. In this discriminant analysis, a linear combination of the independent variables (texture features) is formed and serve as the basis for classifying cases (samples) into one of the groups. Thus, information content in multiple variables is summarized in a single index. The values of the discriminant functions can be estimated from

$$D = B_0 + B_1 X_1 + ... + B_n X_n$$

where the X's are the values of the independent variables and the B's are the weights estimated from the data. The B's are chosen so that the ratio of the between-group sum of squares to the within-group sum of squares (λ) is as large as possible. A good discriminant function is one that has a large between-group variability compared to its within-group variability. It implies that good features should give large λ values.

Based on carcinogenesis, the four groups can be ordered as *normal, regenerating, premalignant*, and *malignant*. To discriminate the different groups in the data set, a hierarchical classification (HC) system was followed, such that the first two steps identify the outter groups, the *malignant* and *normal*, and the third step discriminate the *premalignant* from the *regenerating*.

In the present context, the first step of the HC had two groups, the *malignant* and **non-malignant** (*normal, regenerating* and *premalignant*). The **non-malignant** group was split into two groups in the second step, the *normal* and **non-normal** (*regenerating* and *premalignant*). And the third step had the group *regenerating* and *premalignant*. At each step, the best single and the best combinations of two and three features which discriminated the two respective groups were selected.

This study required evaluation of 30 Laws texture features. So, at each step of the HC, the per-

formance of each single feature was first analyzed by the λ values. Since the total number of features is quite large (30), only the 15 best features were selected for the feature combination process.

The best combination of two and three features were selected by a suboptimal search i.e., the best single feature was combined one by one with the other 14 features to find the best combination of two features, and then the best combination of two was combined one by one with the remaining 13 features to find the best combination of three features.

The correct classification rate (CCR) of the best single and the best combinations of features in the training set was computed by using the Jackknife or Leave-one-out classification method i.e., each case marked as *ungrouped* was classified into the group with the highest *a posteriori* probability according to the discriminant function.

The discriminating power of the best combinations of features was tested on the independent test set. All the cases in the test set were marked as *ungrouped* and the group membership was predicted by the discrimination function computed using the best combinations of features obtained from the training set. The number of cases classified correctly represented the CCR for the test set.

5 Results

5.1 Step-1 of HC

The first step had two groups, the *malignant* and **non-malignant**, where the *malignant* consisted of 5 samples and the **non-malignant** (*normal*, *regenerating*, and *premalignant*) consisted of 15 samples in the training set. The best single and the best combination of two and three features which discriminated the *malignant* group from the **non-malignant** group were selected, and their CCR's are presented in Table 3.

The discrimination function based on the best set of 3 features (A, B, and C; see Table 2) clearly identified the *malignant* group (CCR=100%). None of the samples were misclassified. Once we selected the features which identified the *malignant* group, we proceded to step-2.

5.2 Step-2 of HC

Here, we worked with the *normal* group, consisting of 5 samples, and the **non-normal** group (*regenerating* and *premalignant*) consisting of 10 samples in the training set. The features D, E, and F (see Table 2), which totally discriminated the *normal* group from the **non-normal** group in the training set, were selected. Table 4 presents the CCR's for these features. All the samples from both groups were correctly classifed (CCR=100%) by the three features.

Notation	Feature
A	$M6_{PA}$
B	$M5_{PA}$
C	$M1_{\sigma}$
D	$M4_{\mu}$
E	$M4_{PA}$
F	$M5_{AA}$
G	$M4_{AA}$
H	$M1_{AA}$
I	$M4_{\sigma}$

Table 2: *The notation of the features which have been selected in all three steps in the HC system.*

Feature	CCR in %	
	Malignant	Non-Malignant
A	80	80
A+B	80	87
A+B+C	100	100

Table 3: *The CCR's for the best single, the best combination of two and three features which discriminated the malignant group from the* **non-malignant** *(normal, regenerating and premalignant) in the training set.*

After the first two steps, we were able to identify the *malignant* and the *normal* groups from the *premalignant* and *regenerating* groups.

Feature	CCR in %	
	Normal	Non-Normal
D	60	80
D+E	80	80
D+E+F	100	100

Table 4: *The CCR's for the best single, the best combination of two and three features which discriminated the group normal from the* **non-normal** *group (regenerating and premalignant) in the training set.*

5.3 Step-3 of HC

We ended up with two groups, the *regenerating* and the *premalignant*, at the third step. The training set had 5 samples from each of the two groups. The selected features G, H, and I (see Table 2)

correctly classified all the samples from the *regenerating* group (CCR=100%), and misclassified one sample from the *premalignant* group as *regenerating* (CCR=80%) in the training set, see Table 5.

Feature	CCR in %	
	Regen	Premal
G	100	80
G+H	100	80
G+H+I	100	80

Table 5: *The CCR's for the best single, the best combination of two and three features which discriminated the group regenerating from the group premalignant in the training set.*

5.4 Test set

The best combination of three features which discriminated the two respective groups in each step of the HC were then tested on the independent data set to see if the combinations perform well enough to be useful.

The first step of the HC had 6 samples from the *malignant* and 10 from the *premalignant* group in the test set. The feature combination A, B, and C correctly identified the six samples as *malignant* (CCR=100%), and classified all the samples from *premalignant* as **non-malignant** (CCR=100%), see Table 6.

The test set in the second step consisted of 10 samples from the *premalignant* group. The feature combination D, E, and F, which discriminated the *normal* from the **non-normal** (*regenerating* and *premalignant*), correctly identified the ten samples as **non-normal** (CCR=100%), see Table 6.

The two groups in the third step were the *regenerating* and *premalignant*, and the test set had 10 samples from the *premalignant*. The features G, H, and I together correctly identified all the samples (CCR=100%), see Table 6.

Feature	Step-1	
	Malignant	Non-Malignant
A+B+C	100%	100%
	Step-2	
	Normal	Non-normal
D+E+F	-	100%
	Step-3	
	Regeneratin	Pre-malignant
G+H+I	-	100%

Table 6: *The CCR's for the best combination of three features which discriminated the two respective groups at each step of the HC in the test set.*

6 Discussion

As far as we know, there have been two prior TEM studies based on texture analysis, except for the studies performed in our own group. Auger et. al. [3] have used five shape and texture parameters to compute a discriminant function for the classification of human sperm cell nuclei during differentiation and maturation. Kriete et. al. [7] have analyzed area, form factor, and texture parameters from second derivative images in order to differentiate thyroid gland tumors and found differences between these lesions. However, non of the studies were confirmed with an independent test set.

Previous studies in our group using TEM images of liver cell nuclei ([5], [6], [1], [2], [11], [4], [9], [12]) have shown that the chromatin texture features are important discriminating parameters in liver carcinogenesis. Yogesan et. al. [12] used three different texture estimators, GLCM, GLRLM, Gray Level Variance Matrix(GLVM), to discriminate the four different groups simultaneously. The performance of the selected texture features were tested on the independent test set.

In this study we applied Laws masks, which is simple and easy for computation, to extract features from the cell nucleus region. We followed a hierarchical classification system, which does the discrimination stepwise, to identify early as well as late stage of malignancy.

The goal of this study is the identification of *normal, premalignant* and *malignant* liver cells. Using Laws texture features and following a HC system on the training set clearly indicates the possibility of achieving the goal, and the feature performance on the independent test set further strengthen it.

The three features S3E3/E3S3$_{PA}$, S3L3/L3S3$_{PA}$, and L3L3$_{\sigma}$ used in the first step, clearly identified the *malignant* samples from the **non-malignant** with 100% CCR both in training and test. This result indicats that these features were able to separate the *malignant* from the *premalignant*, and therfore the features could be used to identify the late stage of liver carcinogenisis. However, the first step did not attempt to identify the *premalignant* from the *normal* and *regenerating*.

The second step partly achieved this by the feature combination L3E3/E3L3$_{\mu}$, L3E3/E3L3$_{PA}$, and L3S3/S3L3$_{AA}$, which successfully distinguished the

normal samples from the *premalignant* and *regenerating*, giving a 100% CCR in the training set and the test set. The results of the two steps showed that we were able to clearly identify the two outter groups. And at the third step, the features L3E3/E3L3$_{AA}$, L3L3$_{AA}$, and L3E3/E3L3$_{\sigma}$ correctly classified the *regenerating* samples and misclassified one sample from the *premalignant*, which lead to a 90% overall CCR in the training set. However, the features performed well, 100% CCR, in the test set.

The difference between CCR's in the training and test set demonstrates that the empirical estimate of the true CCR should be interpreted with caution, when the number of samples are fairly small. The classification part of the model is based on the Baye's rule, and assume that the data for all the groups come from multivariate normal populations. Furthermore, we have used a pooled covariance matrix. However, the performance of the model on real data will determine its usefulness [10].

The features obtained from the masks which are transposes of each other were combined to form a directional independent features. It would have been interesting to run the masks in 8 directions, obtained by circular shift, like in the compass operators, to form a directional independent features. It is however not possible, simply because the generation of circular shift masks could not be explained by the convolution concept of Laws.

In this study, we used a *median* filter to remove noise. However, noise removal should ideally be optimized such that the removal is acheived without altering local texture. In the present context, we have neither analyzed the effect of the filtering, nor tried to find the optimal filter.

The results demonstrate the value of following a hierarchical classification system, applying a linear discriminant model using Laws texture features in the early detection of malignancy.

The best criterion for evaluating a method such as the present one is to see whether it can be used to discriminate between cells of different biological conditions. Based on the above concept, work is in progress on analyzing the present method as a diagnostic and prognostic tool in clinical prostate and mamma cancer material.

References

[1] F. Albregtsen, K. Yogesan, G. Farrants, and H. E. Danielsen, *"Texture Discrimination of Normal and Malignant Mouse Liver Cell Nuclei"*, in "Theory and Applications of Image Analysis, Selected Papers from "The 7th Scandinavian Conference on Image Analysis", (P. Johansen and S. Olsen, Eds.) Aalborg, Denmark, 13-16 August 1991, pp. 324-335, World Scientific Publishing Company, 1992.

[2] F. Albregtsen, B. Nielsen and K. Yogesan, *"Fractal Dimension, only a Fraction of the Truth?"*, Proc., 11-th ICPR, VOL 3, pp. 733-736, 1992.

[3] J. Auger, D. Schoevaert, I. Negulesco, and J.P. Dadoune, *"The Nucler Status of Human Sperm Cells by TEM Image Cytometry: Nuclear Shape and Chromatine Texture in Semen samples from Fertile and Infertile Men"*, J Androl. 14, pp. 456-463, 1993

[4] S.Baheerathan, K. Yogesan, F. Albregtsen, and H. E. Danielsen, *"Texture Analysis of Liver Carcinogenesis in Mice based on Laws Convolution Matrices "*, Proc., 11-th NOBIM Conf. , pp. 250-253, 1994.

[5] H. E. Danielsen, G. Farrants, and A. Reith, *"Characterization of Chromatin Structure by Image Analysis - A Method for the Assessment of Changes in Chromatin Organization"* Scanning Microscopy Supplement, Vol. 3, pp. 297-302, 1989.

[6] H. E. Danielsen, *"Premalignant Changes in DNA Organization in Mouse Liver after Diethylnitrosamine Treatment"* Thesis. The Norwegian Radium Hospital and Institute for Cancer Research, Oslo, Norway, ISBN 82-7633-016-9, 1991.

[7] A. Kriete, R. Schaffer, H. Harms, and H.M. Aus, *"On-line Transmission Electron Microscopic Image Analysis of Chromatine Texture for differentiation of Thyroid gland Tumors"* Anal. Quant. Cytol. Histol., Vol 9, No. 3, pp. 268-272, 1986.

[8] K. Laws, *"Textured Image Segmentation"*, USCIPI Report No. 940, Thesis, University of Southern California, 1980.

[9] H. Schulerud, J.M. Carstensen, and H. E. Danielsen, *"Multiresolution Texture Analysis of four classes of Mice liver cells using different cell cluster representations"*, Proc. of 9-th Scandinavian Conference on Image Analysis, Sweden, Vol I, pp. 121-129, 1995.

[10] P.W. Strike, *"Statistical Methods in Laboratory Medicine"*, Oxford, Butterworth-Heinemann Ltd, pp. 398-399, 1991

[11] K. Yogesan, F. Albregtsen, A. Reith and H.E. Danielsen, *"Cooccurrence and Run Length-based Texture Analysis of Experimental Liver Carcinogenesis in Mice"*, Proc. of 8-th Scandinavian Conference on Image Analysis, Norway, Vol I, pp. 227-234, 1993.

[12] K. Yogesan, H. Schulerud, F. Albregtsen, and H.E. Danielsen, *"Ultrastructural Texture Analysis as a Diagnostic Tool in Mouse Liver Carcinogenesis"*, In press, 'Ultrastructural Pathology.